Benchmark Cases

Each of the benchmark cases has gradients in the solution of $\nabla \cdot q$ and all but one of the cases has spatial gradients in at least one field property. The four benchmark cases are as follows:

Benchmark 1: Burns and Christon. This case is described by Burns and Christon (Burns 1997). The case describes a three dimensional cube 1m in length, with a constant temperature and a tri-linearly varying absorption coefficient depicted in figure !!!.

Benchmark2: Michael Modest black parallel plates. This case is described by Modest in section 13 of his Radiation Heat Transfer book (Modest 2003). A gray, non-scattering medium with refractive index n=1 is contained between two infinitely parallel, gray plates. The medium is isothermal at temperature T_m, with constant absorption coefficient, κ. The two plates are both isothermal at temperature T_w, have the same gray-diffuse emissivity ϵ, and are spaced a distance L apart. For this problem, a known analytical solution exists for the radiative heat flux as well as the radiative flux divergence. The analytical solution for the flux divergence is as follows

$$\frac{dq}{d\tau} = \sigma(T_w^4 - T_m^4) * \frac{-2[E_2(\tau) + E_2(\tau_L - \tau)]}{1 + (1/\epsilon - 1)[1 - 2E_3(\tau_L)]},$$

where E_2 and E_3 are exponential functions, defined as follows

$$E_n(\tau) = \int_0^1 \mu^{n-2} e^{-\tau/\mu} d\mu,$$

and μ is defined as $cos(\theta)$.

See Modest figure 13.2 for the general behavior of the exponential functions. This case was used with the following values: $\epsilon = 1$, $\tau_L = 1$, $T_w = 1000K$, $T_m = 1500K$, and $L = 1$m. To model the infinite parallel plates, the four side walls were specified with emissivities of 0, such that they had no emissive contribution, and they allowed the rays to reflect specularly. The two remaining walls had an emissivity of 1.

We found that this case required a greater number of rays to achieve comparable accuracy to the Burns and Christon benchmark. This is due to the fact that a ray striking a reflective wall gives a drastically different result than a ray striking the black plate. Therefore the angular discritization, which is a function of ray number, plays a more important role. A ray-convergence plot is given in Fig. 1.

Benchmark 3: Modified Burns and Christon. This case is has the same properties of the Burns and Christon case with one modification–rather than a constant temperature throughout the domain, the temperature was set as follows

$$T = 1000 abskg$$

where $abskg$ is the absorption coefficient.

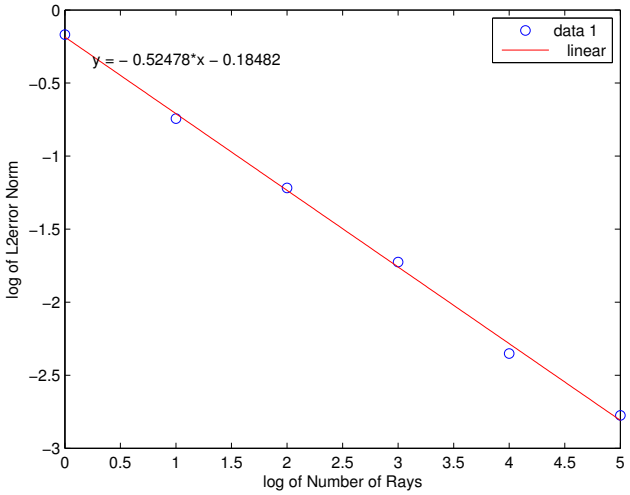

Figure 1: Ray convergence of numerical solution relative to the analytical solution of Benchmark 2. Note that at 100,000 rays, the ray error is approximately $10^{-2.7}$

Benchmark 4: Modified Modest. This case is similar to the Michael Modest case, but with the following two changes.

$$absk g(z) = (\frac{z}{L})^2,$$

$$T = 1000 + 1000 absk g,$$

where z is the vertical coordinate, and L is the length of the domain. Therefore the absorption coefficient changes from 0 to 1 quadratically, and temperature varies from 1000K to 2000K quadratically.

With sufficient ray numbers, however, very good agreement between the numerical and analytical solutions is achievable (see Fig. 2)

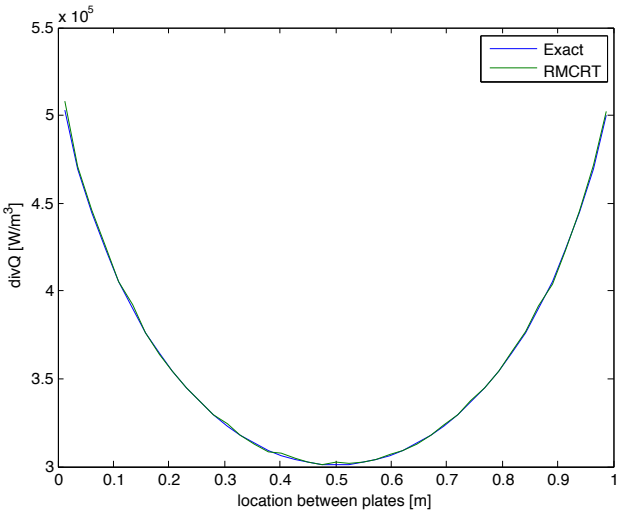

Figure 2: RMCRT shows good agreement with the nalytical solution $\nabla \cdot q$ for the benchmark 2 case.

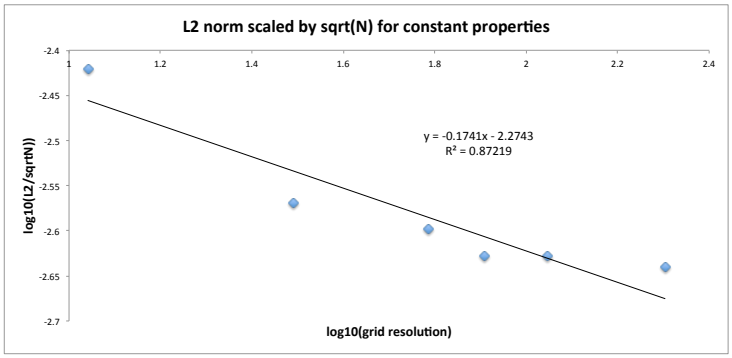

Figure 3: L2 norm of error scaled by $\sqrt{n}$ for benchmark 2. Note that the grid convergence levels off for resolutions greater than approximately 100^3 cells. For resolutions finer than this, the grid error is negligible relative to the ray error, which for this case is approximately $10^{-2.7}$. Also note the shallow slope of convergence even for coarse resolutions. Because the properties of the media do not vary in space, only items 1 and 4 from the theory come into play in grid convergence.

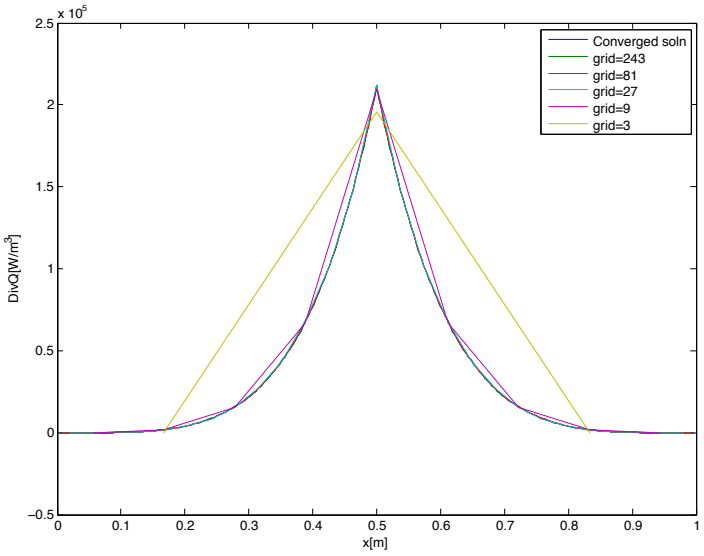

Figure 4: Converged solution of $\nabla \cdot q$ for benchmark 3 vs. $\nabla \cdot q$ from various grid resolutions. Notice that at the locations of interest (cell centers) there is good agreement between the converged solution and even the coarsest meshes. What is not well represented in the coarse meshes, however, is the detail between the cell centers.

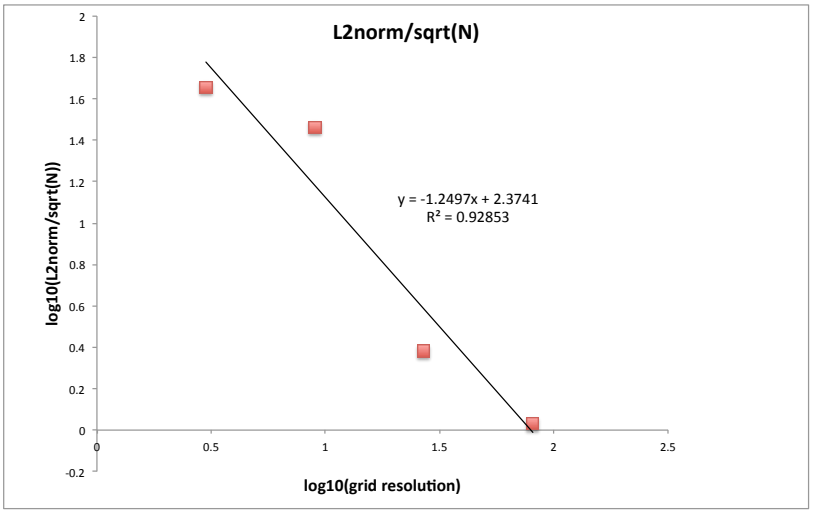

Figure 5: L2 norm of error scaled by $\sqrt{n}$ for benchmark 3. Because this case is based on benchmark 1, which is a symmetric case, we know that the ray error is relatively low, and that the ray convergence rate can be approximated by figure 1. Therefore, there is an increase in accuracy with higher resolutions up and including 81^3.

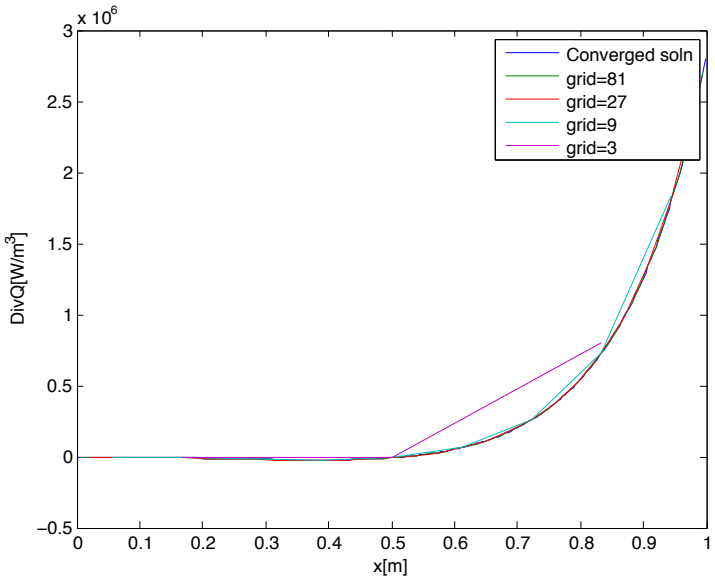

Figure 6: Converged solution of $\nabla \cdot q$ for benchmark 4 vs. $\nabla \cdot q$ from various grid resolutions. Similar to Fig. 4, at the locations of interest (cell centers) there is good agreement between the converged solution and even the coarsest meshes, but between the cell centers, detail is lost.

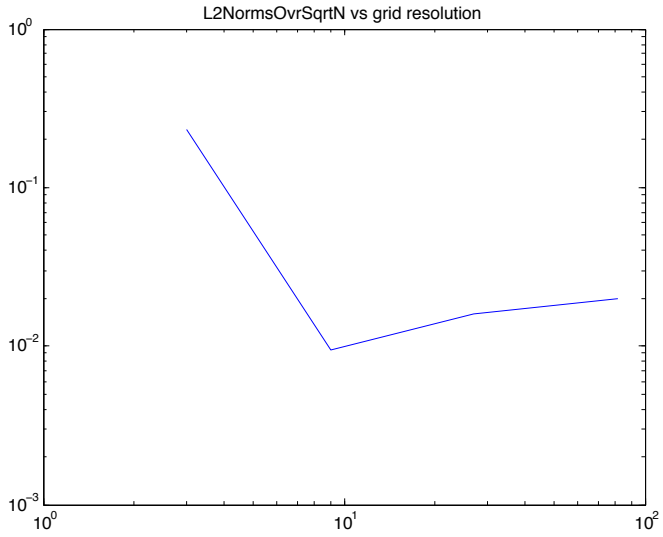

Figure 7: L2 norm of error scaled by $\sqrt{n}$ for benchmark 4. Because the result of ray striking a reflective surface is so different from the result of a ray striking a black plate is so drastically different, the ray error is quite high even for large numbers of rays (100,000 in this case). This is demonstrated by the fact that there is no increase in accuracy beyond even 9^3 cells.

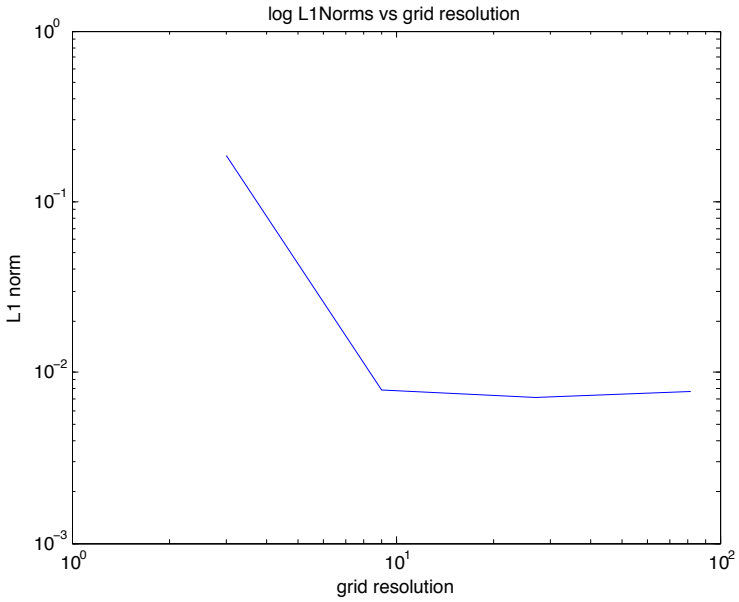

Figure 8: L1 norm of error scaled by N for benchmark 4. This figure is mostly redundant to the previous figure, but demonstrates the lack of increase in accuracy for increased resolution.